present findings indicate that cyclodextrins are excellent models of hydrolytic enzymes.

Acknowledgment. This work was supported by grants from the National Science Foundation and the Hoffmann-La Roche Inc.

References and Notes

(1) S. S. Biechler and R. W. Taft, Jr., *J. Am. Chem. Soc.*, **79**, 4927 (1957).
(2) M. L. Bender and R. J. Thomas, *J. Am. Chem. Soc.*, **83**, 4183 (1961).
(3) P. M. Mader, *J. Am. Chem. Soc.*, **87**, 3191 (1965).
(4) S. O. Eriksson and C. Holst, *Acta Chem. Scand.*, **20**, 1892 (1966).
(5) S. O. Eriksson and L. Bratt, *Acta Chem. Scand.*, **21**, 1812 (1967).
(6) R. M. Pollack and M. L. Bender, *J. Am. Chem. Soc.*, **92**, 7190 (1970).
(7) C. O'Connor, *Q. Rev., Chem. Soc.*, **24**, 553 (1970).
(8) R. H. DeWolfe and R. C. Newcomb, *J. Org. Chem.*, **36**, 3870 (1971).
(9) C. E. Stauffer, *J. Am. Chem. Soc.*, **94**, 7887 (1972).
(10) R. M. Pollack and T. C. Dumsha, *J. Am. Chem. Soc.*, **95**, 4463 (1973).
(11) R. L. Schowen and G. W. Zuorick, *J. Am. Chem. Soc.*, **88**, 1223 (1966).
(12) R. L. Schowen, H. Jayaraman, and L. Kershner, *J. Am. Chem. Soc.*, **88**, 3373 (1966).
(13) R. L. Schowen, H. Jayaraman, L. Kershner, and G. W. Zuorick, *J. Am. Chem. Soc.*, **88**, 4008 (1966).
(14) L. D. Kershner and R. L. Schowen, *J. Am. Chem. Soc.*, **93**, 2014 (1971).
(15) V. Gani and P. Viout, *Tetrahedron Lett.*, 5241 (1972).
(16) M. L. Bender and M. Komiyama in "Bioorganic Chemistry", Vol. I, E. E. van Tamelen, Ed., Academic Press, New York, N.Y., 1977, Chapter 2.
(17) R. L. VanEtten, J. F. Sebastian, G. A. Clowes, and M. L. Bender, *J. Am. Chem. Soc.*, **89**, 3242 (1967).
(18) R. L. VanEtten, G. A. Clowes, J. F. Sebastian, and M. L. Bender, *J. Am. Chem. Soc.*, **89**, 3253 (1967).
(19) D. E. Tutt and M. A. Schwartz, *J. Am. Chem. Soc.*, **93**, 767 (1971).
(20) M. Komiyama and M. L. Bender, *Bioorg. Chem.*, in press.
(21) M. J. Saxby, *Org. Mass Spectrom.*, **2**, 835 (1969).
(22) P. K. Glasoe and F. A. Long, *J. Phys. Chem.*, **64**, 188 (1960).
(23) H. A. Benesi and J. H. Hildebrand, *J. Am. Chem. Soc.*, **71**, 2703 (1949).
(24) M. Komiyama, E. J. Breaux, and M. L. Bender, *Bioorg. Chem.*, **6**, 127 (1977).
(25) K. A. Connors and J. M. Lipari, *J. Pharm. Sci.*, **65**, 379 (1976).

Interaction of Cis Platinum(II) Compounds with Poly(L-glutamate). A Doubly Anchored Spin-Label and a Doubly Anchored Chromophore-Label[1]

Yen-Yau H. Chao, Alfred Holtzer,*[2] and Stephen H. Mastin

Contribution from the Department of Chemistry, Washington University, St. Louis, Missouri 63130. *Received December 20, 1976*

Abstract: The free-radical 4-amino-2,2,6,6-tetramethylpiperidinyl-1-oxy (ATMPO) yields *cis*-Pt(ATMPO)$_2$(NO$_3$)$_2$, which is used to label poly(L-glutamate) [(Glu)$_n$], poly(L-aspartate) [(Asp)$_n$], and poly(L-lysine) [(Lys)$_n$]. Labeling occurs by displacement of nitrate by polymer side chains. Electron spin resonance (ESR) spectra of oriented films of labeled (Glu)$_n$ are strongly anisotropic; several arguments suggest that the major cause is g anisotropy. Spectra of solutions, in several solvents, of labeled (Glu)$_n$ are also anisotropic and monitor the helix-coil transition and polymer aggregation. Since monofunctional, side-chain labels show only isotropic motions, Pt must be bifunctionally anchored to adjacent carboxylates, requiring the label to follow backbone segmental motions. With shorter side chains [(Asp)$_n$], adjacent double anchoring is impossible; with longer side chains [(Lys)$_n$], flexibility reduces coupling to backbone motion; in each, therefore, spectra are isotropic. Chromophoric compounds, particularly [*cis*-Pt(bpy)(H$_2$O)$_2$][NO$_3$]$_2$, are similarly used. Bifunctional attachment is evidenced by the absence of base-induced ultraviolet (UV) spectral shifts (characteristic of attachment of OH$^-$ to Pt) shown by label alone, and by similarity of the spectra of labeled polymer and labeled oxalate. Induced circular dichroism (CD) appears for α helix in the region of the chromophore π-π^* bands; transition to random coil drastically reduces this CD. With extensively labeled polymer, differences in the course of the helix-coil transition as monitored by CD in the backbone region with that monitored in the chromophore region show that the label stabilizes its attached helical residue. A study of Corey-Pauling-Koltun (CPK) models and extant theories suggests that the induced CD arises by coupling of the carboxylate π-π^* and the bound chromophore $^1B_1$ electric transition moments.

Spin-labels have been widely used in a variety of systems. The resulting ESR spectra presumably contain information on the mobility of the host macromolecule. However, since the attachment of the label is usually monofunctional, the spectra often also strongly reflect the more or less independent motion of the spin-label itself. In many cases, it is impossible to sort out the various motional contributions to the spectrum. For example, an ordinary monofunctional spin-label attached to a side chain of poly(L-glutamate) [which we sumbolize (Glu)$_n$] gives an unrevealing, rather mobile, spin spectrum.[3] Hitherto, only in one very special case, in which a monofunctional label was rather *rigidly* attached to the carboxyl end group of poly(benzyl-L-glutamate),[4] has it been found that the ESR spectrum of a synthetic polypeptide is sensitive to the anisotropic motion that should be characteristic of the macromolecule itself.

We describe here an attempt to eliminate, or at least decrease, the complications ascribable to independent motion of the spin-label by employing a side-chain spin-label that is anchored to the macromolecule at *two* points and is thus required to follow more closely the segmental motion of its host. We therefore synthesized, and used as a label for (Glu)$_n$, the biradical platinum *cis*-(4-amino-2,2,6,6-tetramethylpiperidinyl-1-oxy) dinitrate [called *cis*-Pt(ATMPO)$_2$(NO$_3$)$_2$]:

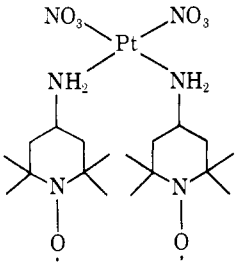

We were hopeful that the carboxylate side chains on the (Glu)$_n$ polymer would be favorably suited to displace the nitrates, resulting in a bifunctionally labeled macromolecule.

We report here experiments suggesting that such bifunctionally anchored spin-labeling of $(Glu)_n$ does indeed take place and that the ESR spectra reflect those changes in macromolecular segmental motions that accompany both the helix–coil transition and polymer aggregation. Some additional results on labeled poly(L-aspartate) [called $(Asp)_n$] and poly(L-lysine) [called $(Lys)_n$] serve to define the limitations of the method, and are reported for comparison.

In a similar way, it is possible to attach chromophore-bearing Pt(II) compounds to $(Glu)_n$ and to examine the resulting absorption spectra of the labeled polymer. Moreover, the possibility exists that binding of a symmetric, optically inactive chromophore to a dissymmetric polypeptide will induce optical activity in the chromophore absorption regions of the spectrum, prompting examination also of the circular dichroism (CD) spectrum of the labeled polymer. If such Pt(II) compounds are indeed bifunctionally attached, and therefore forced to follow host segmental movements, then host conformational transitions should also be reflected in changes in the CD spectrum, if any, in the region of the chromophore absorption.

To further test these ideas, we synthesized three chromophore-bearing cis Pt(II) compounds: *cis*-$Pt^{II}(py)_2(NO_3)_2$ (**1**); $[Pt^{II}(bpy)(H_2O)_2][NO_3]_2$ (**2**); and $[Pt^{II}(phen)(H_2O)_2][NO_3]_2$ (**3**). These were then bound to $(Glu)_n$ and absorption

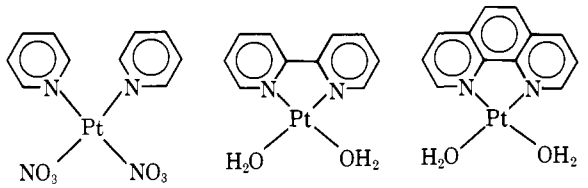

1 2 3

and circular dichroism spectra taken in the region of the π–π^* transition bands of the chromophore.

As will be seen, these experiments with chromophore labels confirm the picture of the bifunctional binding suggested by the spin-label results, show that binding to the macromolecule induces optical activity in the chromophore absorption region, and indicate that the induced optical activity is not only sensitive to macromolecular conformations, but also influences their relative stability. The electrical origins of the induced optical activity are briefly discussed in terms of available theory, and some tentative assignments made.

Experimental Section

Chemicals and Physical Measurements. The ATMPO used in synthesizing the biradical was from Aldrich Chemical Co. Two sources of $(Glu)_n$ were used: the acid form, from Pilot Chemical, and the sodium salt, from Sigma Chemical; no differences in behavior were observed. $(Asp)_n$ was obtained as the potassium salt from Pilot Chemical. $(Lys)_n$ was obtained as the hydrobromide from Schwarz/Mann. Molecular weights (as supplied by the manufacturer) of all polymers were near 60 000. Other common chemicals were reagent grade, and were used without further purification. For all experiments, distilled water was passed through charcoal and mixed-bed ion-exchange resin columns before use.

The ESR spectrometer used has already been described.[5,6] Absorption and CD spectra were taken on a Durrum-Jasco Model J-20 spectrophotometer.

Synthesis of Labels. Reaction of ATMPO with K_2PtI_4 produced *cis*-$Pt(ATMPO)_2I_2$ (two intense Raman Pt–I stretching bands at 153 and 182 cm^{-1}) in 90% yield as a light brown powder, mp 244 °C dec. Reactions of the latter compound with $AgNO_3$ in acetone–ethanol gave *cis*-$Pt(ATMPO)_2(NO_3)_2$ (IR, monocoordinated nitrato: 1500, 1290, 960 cm^{-1}) in 90% yield as colorless plates, mp 135 °C. Complexes were purified (only one component detectable by thin-layer chromatography (TLC)) by column chromatography [silica gel; 3:2 (v/v) benzene–chloroform eluent] and/or careful fractional recrystallization from acetone. The nitrate was used for labeling experiments

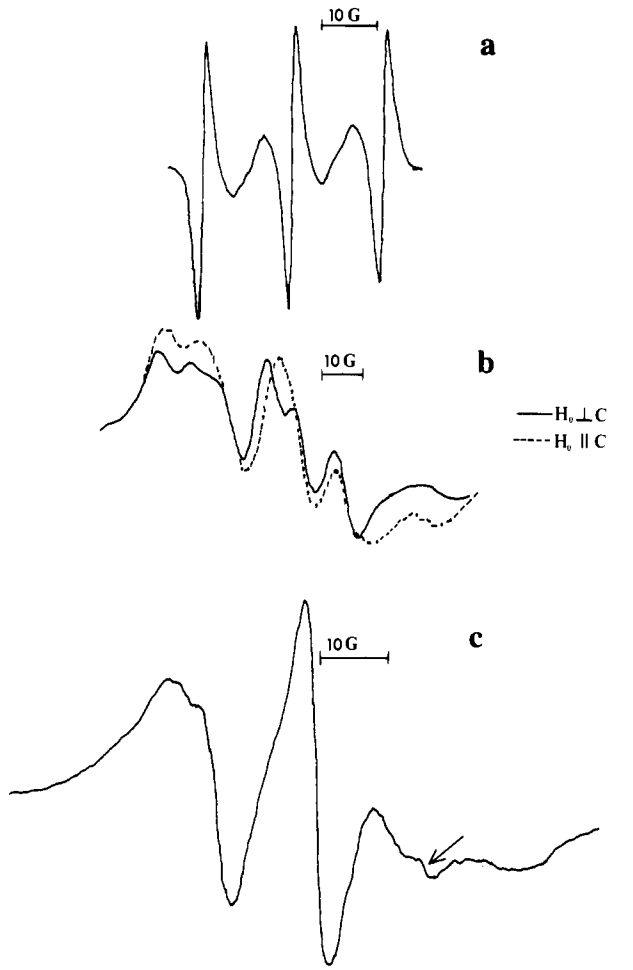

Figure 1. (a) ESR spectrum of *cis*-$[Pt(ATMPO)_2(H_2O)_2^{2+}](NO_3^-)_2$ in water. (b) ESR spectra of oriented film of $(Glu)_n$ labeled with [*cis*-$Pt(ATMPO)_2]^{2+}$. Only about one $(Glu)_n$ molecule in every four is labeled and on labeled molecules only 1 side chain in every 20 is labeled. Solid curve is for external field perpendicular to *C* axis of film, dashed curve for external field parallel to *C* axis. (c) ESR spectrum of $(Glu)_n$ labeled with [*cis*-$Pt(ATMPO)_2]^{2+}$; polymer is in dimethylformamide solution at 10% concentration. Arrow marks position of a small peak due to mobile spins.

because of its ready solubility in water. Its ESR spectrum in aqueous solution (Figure 1a) shows the same characteristic sharp triplet as the parent ATMPO; in addition, broad resonances between the central peak and each of the outer peaks of the triplet are clearly due to electron–electron exchange and thus confirm the biradical nature and cis geometry of the complex.

Chromophore-label compound **1** was made from a sample of *cis*-$Pt^{II}(py)_2Cl_2$ that had itself been synthesized by known methods.[7] Solid $AgNO_3$ was added to an aqueous suspension of the sparingly soluble chloride. The vessel was wrapped to prevent photochemical decomposition, and the suspension stirred for 1 day. The clear supernatant containing the soluble nitrate compound was removed and lyophilized, allowing collection of **1** as a white powder. Compound **1** is quite soluble in water.

Chromophore-label compounds **2** and **3** were prepared by methods similar to those used for **1**. The analogous chloride starting materials were synthesized and graciously supplied to us by Dr. PO-Hsin Liu. In the preparation of **2** and of **3**, reaction with $AgNO_3$ was slow and was allowed to continue for 4 to 7 days. After centrifugation, the supernatant was lyophilized and **2** (or **3**) collected as a yellowish powder. Both compounds are moderately soluble in water. The coordination of water in the solid compounds **2** and **3** was confirmed by infrared spectroscopy (also graciously done by Dr. Po-Hsin Liu): a strong water band is seen along with N–O stretching bands that do not show the splitting characteristic of coordinated nitrate.

Labeling of the Macromolecules. Spin-labeling of polymers was accomplished in most experiments by addition of sufficient solid

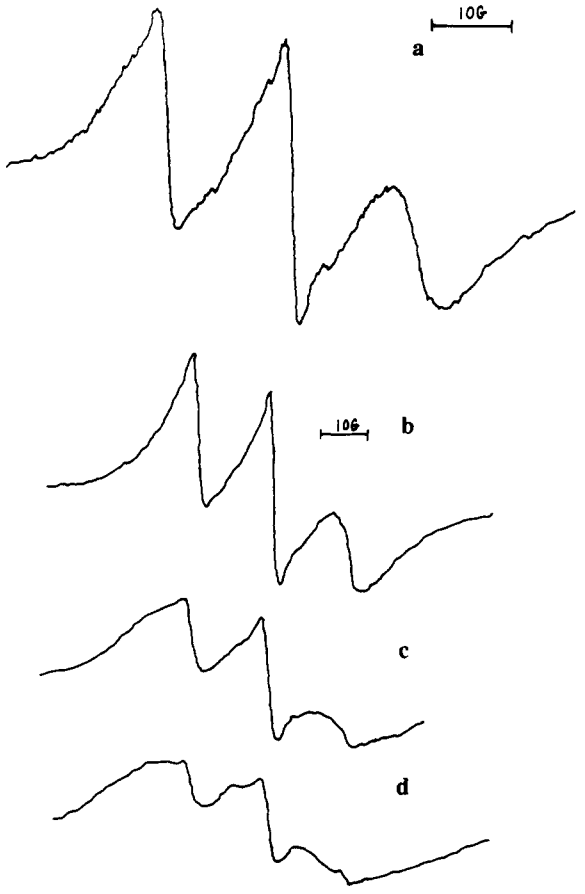

Figure 2. ESR spectra at various pHs of $(Glu)_n$ labeled with [*cis*-$Pt(ATMPO)_2]^{2+}$; polymer is in aqueous 0.2 M $NaNO_3$ solution at (a) pH 8.0; (b) pH 5.1; (c) pH 4.3; (d) pH 4.0.

cis-$Pt(ATMPO)_2(NO_3)_2$ to a 0.4–0.6% polymer solution to bring the molar concentration of label to 5% of the residue molar concentration of the polymer. Reaction was allowed to proceed for 8 h at 25 °C. Dialysis then followed, although our experience with the chromophoric labels (see below) indicates that the label reacts essentially quantitatively and nondialyzably, at least with $(Glu)_n$. For aqueous polymer solutions, labeling was usually performed at pH 6.4 at which $(Glu)_n$, $(Asp)_n$, and $(Lys)_n$ are randomly coiled. However, $(Glu)_n$ spin-labeled while in the helical form (in water or in dimethylformamide) gives the same ESR spectra. Thus, the same labeled product results regardless of whether helix or coil is labeled. For experiments on aqueous media, salts and anions (e.g., halides) that compete with polymer for Pt sites are to be avoided; consequently, we employed $NaNO_3$ as supporting electrolyte where needed.

Chromophore-labeling was performed essentially as described for spin-labeling, except that usually only enough chromophore-containing compound was added to react with 2–4% of the polymer side chains. The reaction is almost quantitative, as judged by the ultraviolet absorbance in the chromophore region before and after dialysis. Since compounds **2** and **3** precipitate readily when their coordinated water is displaced, competing ligands are to be avoided; hence, we employed, where needed, $NaNO_3$ as supporting electrolyte and HNO_3 for acidification. Alkalization, if necessary, was effected with NaOH.

Preparation or Oriented $(Glu)_n$. A 10% solution of the acidic form of $(Glu)_n$ in dimethylformamide was first prepared. The $(Glu)_n$ was spin-labeled as described above. After dialysis, sufficient unlabeled, solid $(Glu)_n$ was dissolved in the solution to bring the total $(Glu)_n$ concentration to 40%. This additional polymer serves to separate spin-labeled molecules in the final oriented film. The addition is made after dialysis because dialysis of a 40% solution results in pronounced swelling of the bag. The viscous solution was then spread onto the ESR sample holder plate (the Teflon sample holder used for oriented samples has been described previously[5]) and a flat spatula used to stroke the oriented film that forms through partial drying. The glass cover[5,6] prevents further drying. The calibration of the field for ESR spectra was accomplished by taping a small capillary tube containing an aqueous solution of the standard radical 2,2,5,5-tetramethyl-3-carbamidopyrrolidinyl-1-oxy to the opposite side of the sample holder.

Results

A. Spin-Labels. 1. Oriented $(Glu)_n$. Examples of ESR spectra of an oriented sample are presented in Figure 1b. The film was stroked in a direction perpendicular to the axis of the ESR cell. In the oriented phase, of course, the long axis of a given helical $(Glu)_n$ molecule is preferentially oriented in the direction of stroking, referred to as the *C* axis.[8] Spectra are shown for the magnetic field parallel to and perpendicular to the *C* axis. The spectrum is clearly dependent upon the orientation of the *C* axis with respect to the magnetic field. Furthermore, although both orientations show some splitting of the hyperfine lines, it is particularly apparent from the central peak that the splitting is pronouncedly larger, especially for the central peak, in the perpendicular orientation. On the other hand, films prepared by stroking in a direction parallel to the axis of the ESR cell must always have *C* axes perpendicular to the magnetic field. As expected, such samples show spectra resembling the solid curve of Figure 1b whatever the orientation about the cell axis.[6]

2. $(Glu)_n$ in Dimethylformamide. The ESR spectrum of a labeled $(Glu)_n$ in dimethylformamide, a strongly helicogenic solvent, is shown in Figure 1c. With the exception of the very small, superposed sharp peak (indicated by the arrow) that indicates isotropic spins, the spectrum clearly shows evidence that the spins, bound to helical $(Glu)_n$ molecules, undergo strongly anisotropic motions. The spectrum is, in fact, strikingly similar to that observed (see Figure 1 of ref 4) for solutions of a rigidly end-labeled, helical poly(benzyl-L-glutamate), and was originally interpreted as arising as a simple consequence of an effective Hamiltonian having axial symmetry,[4] but has since been shown to possess features sensitive to rotations about the C–N (4-amino nitrogen) bond as well.[9]

3. $(Glu)_n$ in Pure and in Mixed Aqueous Solvents. ESR spectra of labeled $(Glu)_n$ in 0.2 M $NaNO_3$ solutions at several pH values are shown in Figure 2. The pH range was selected to sample the coil region (pH >5.4), the helix–coil transition region (pH ~4.8–5.4), the helix region (pH ~4.2–4.8), and the aggregated-helix region (pH <4.2).[10] In none of these, not even in the random-coil region, is the spectrum characteristic of a free spin, such as one finds for ordinary spin-labels on this polymer.[3]

Since the $(Glu)_n$ helix is stronger in dimethylformamide than in water, it is desirable to see what effect the former solvent has on the spectrum. Consequently, we studied the labeled polymer in 50:50 (v/v) mixtures of dimethylformamide and water. The resulting spectra are shown in Figure 3 for nominal pHs (i.e., those read from a pH meter calibrated, in the conventional manner, for use on aqueous solutions) of 3.3 and 7.7. This range of nominal pH essentially spans the helix–coil transition region in this medium (see below). Furthermore, in the mixed solvent, there is no precipitation even at nominal pHs as low as 2.0, so that there is, in all likelihood, no aggregation such as is observed in purely aqueous media. Figure 3 clearly shows not only that a marked change in spectrum accompanies the conformational transition in the mixed solvent, but also that (if one ignores the small contribution from mobile spins, marked with arrows on the figure) there is a strong similarity between the spectra of the helical forms in the mixed solvent (Figure 3b) and in pure dimethylformamide (Figure 1c); both display features characteristic of strongly anisotropic motion.

4. $(Lys)_n$ and $(Asp)_n$ in Aqueous Solvent. Spectra of labeled $(Lys)_n$ in water are shown in Figure 4 for both the randomly coiled (pH 6) and helical (pH 11) conformations. Although

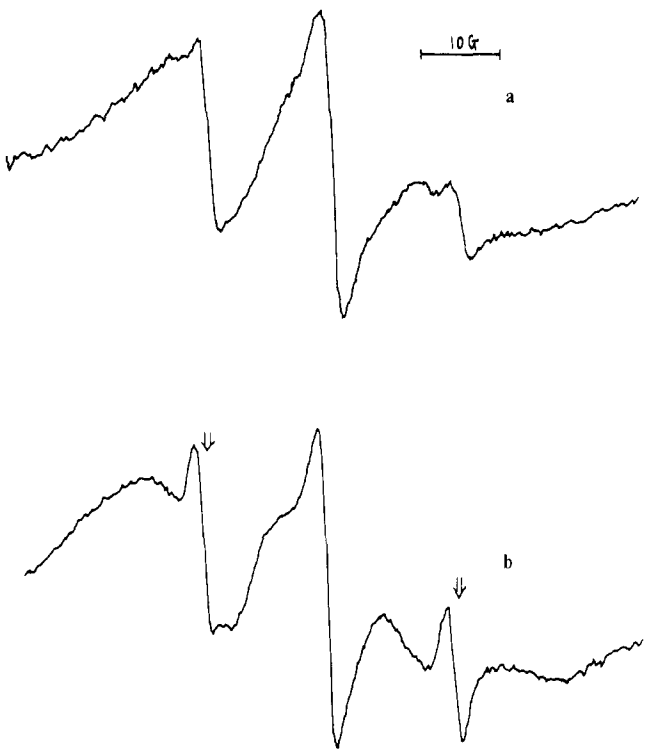

Figure 3. ESR spectra at two pHs of $(Glu)_n$ labeled with [*cis*-$Pt(ATMPO)_2]^{2+}$; polymer is in 50:50 (v/v) mixture of water and dimethylformamide. Arrows mark locations of peaks due to mobile spins: (a) nominal pH 7.7; (b) nominal pH 3.3.

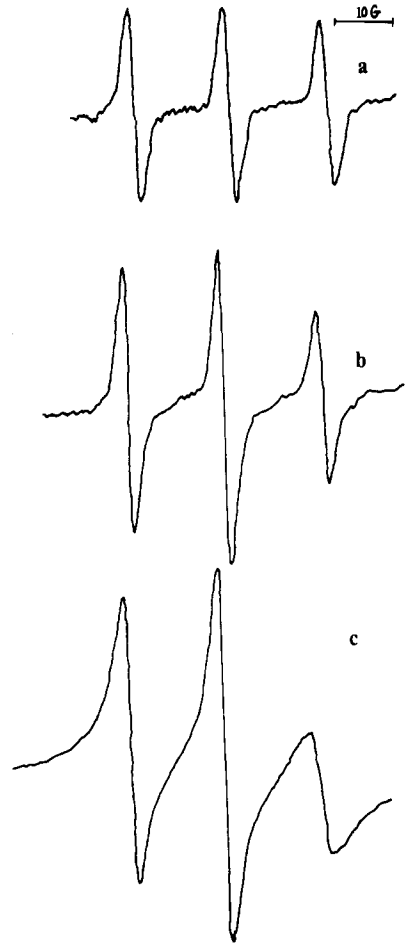

Figure 4. ESR spectra at two pHs of $(Lys)_n$ or $(Asp)_n$ labeled with [*cis*-$Pt(ATMPO)_2]^{2+}$. $(Lys)_n$ is in water at: (a) pH 6.0; (b) pH 11; (c) $(Asp)_n$ is in water at pH 7.2.

the line widths in the two spectra are not identical, both spectra are, in general form, characteristic of spins that are only weakly immobilized. This is in strong contrast to the results for labeled $(Glu)_n$.

Similarly, the spectrum of labeled $(Asp)_n$ (Figure 4c) shows only loose spins. The spectrum displayed is for $(Asp)_n$ in the randomly coiled form, but reduction of the pH to as low as 3.6, which produces partially helical forms, did not alter the spectrum.

B. Chromophore Labels. 1. UV Spectra of Labels and of Labeled Compounds. Spectra of compounds **1**, **2**, and **3** in acidic aqueous solution are shown in Figure 5. The long-wavelength π–π^* transition bands[11-15] of compound **1** and of compound **3** appear at ~250–280 and at ~260–290 nm, respectively. These are not very well resolved from the long-wavelength tail of the longest wavelength backbone CD peak of $(Glu)_n$, which is at ~220 nm. On the other hand, the π–π^* band ($^1B_1$ band[15]) of **2** lies in the ~300–330-nm region, rather far from the polypeptide backbone bands. Consequently, in most of our labeling experiments we used compound **2**.

Since variation of pH is to be employed to alter the $(Glu)_n$ conformation, it is necessary to examine the effect of pH on the spectrum of the label itself. Ultraviolet spectra of compound **2** at various pHs are shown in Figure 6. As pH is increased, the shorter wavelength transition bands borrow a lot of intensity from the 300–330-nm ligand band, undoubtedly as a result of coordination of OH^- at the higher pHs. We have also observed drastic changes with pH for compounds **1** and **3**.

When the label is attached to $(Glu)_n$, its UV spectrum (Figure 7a) matches that of low pH solutions of the unattached label, as can be seen by comparing Figure 7a with Figure 6. Furthermore, we found the spectrum of the $(Glu)_n$-attached label to be independent of pH in the range where the unattached label shows drastic changes, suggesting immediately that the side chains of $(Glu)_n$ prevent attachment of OH^- to the Pt, i.e. that the label is bifunctionally attached to the polymer. This is supported by experiments such as the one illustrated in Figure 7b in which spectra for $(Glu)_n$ labeled with **1** and oxalate labeled with **1** are each displayed. The spectra are barely distinguishable, arguing strongly that the label is attached to $(Glu)_n$ in the same way as it is to oxalate.

2. CD Spectra of Labeled $(Glu)_n$. CD spectra in the region of the label bands are shown in Figure 8a as a function of pH for aqueous solutions of $(Glu)_n$ labeled with compound **2**. There is a strong negative band at ~306 nm, a shoulder at ~317 nm, and a broad band at ~350 nm, all of which match well with the peaks found in the UV spectrum (Figure 7a). Compound **2** itself is, of course, optically inactive; furthermore, mixtures of it with monomeric sodium L-glutamate showed no CD spectrum in the chromophore absorption region.

With increasing pH, the $(Glu)_n$ undergoes the helix–coil transition, a process that results, as is seen in Figure 8a, in a marked decrease in the intensity of the chromophore CD bands. Essentially the same results are obtained with labeled $(Glu)_n$ dissolved in mixtures of dimethylformamide and water, as is shown in Figure 8b.

Furthermore, these CD spectra of $(Glu)_n$ labeled at low molar ratios of label to glutamate residues were found to be independent of that ratio within wide limits. This rules out the possibility that coupling between chromophores is involved; the induced optical activity must be caused by interaction of the label with the dissymmetric polymer.

On the other hand, *extensive* labeling of the polymer, although it does not alter the nature of the CD spectrum, does render it independent of pH by preventing the helix–coil

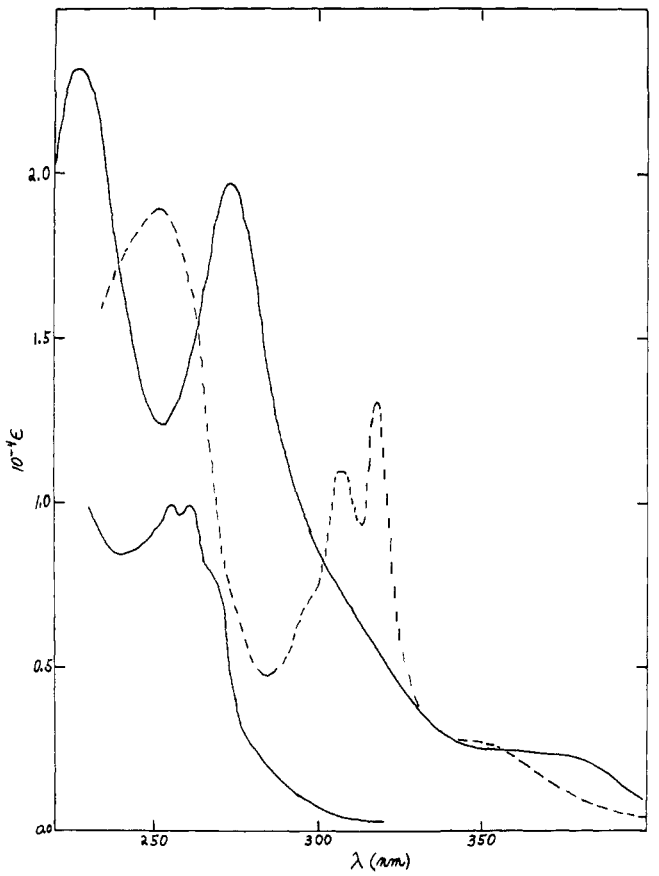

Figure 5. UV absorption spectra of chromophore labels in water at pH 3. Lower solid curve is **1**; dashed curve is **2**; upper solid curve is 3.

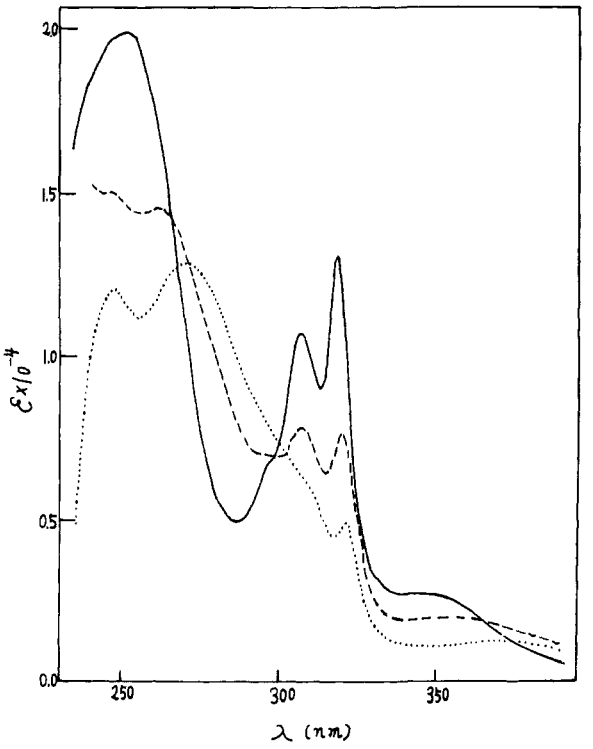

Figure 6. UV absorption spectra of chromophore **2** in water at various pHs. Solid curve, pH 4.9; dashed curve, pH 7.8; dotted curve, pH 10.7.

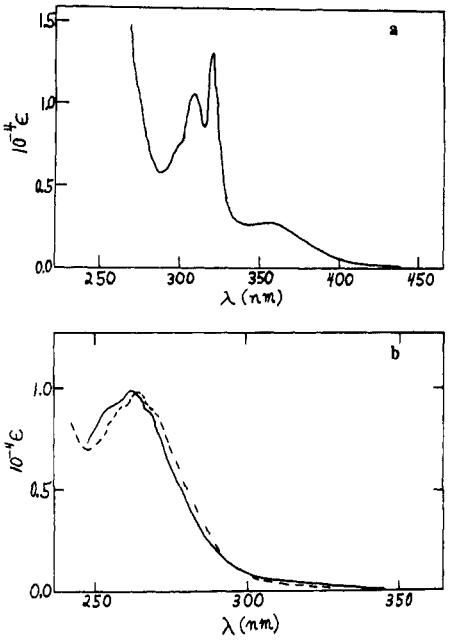

Figure 7. UV absorption spectra of chromophore-labeled compounds. (a) $(Glu)_n$ labeled with **2**; spectrum is for water solution at pH 5.5. (b) Solid curve, pH 7 aqueous solution of oxalate labeled with **1**, i.e., $Pt(py)_2(ox)$; dashed curve, pH 7 aqueous solution of $(Glu)_n$ labeled with **1**.

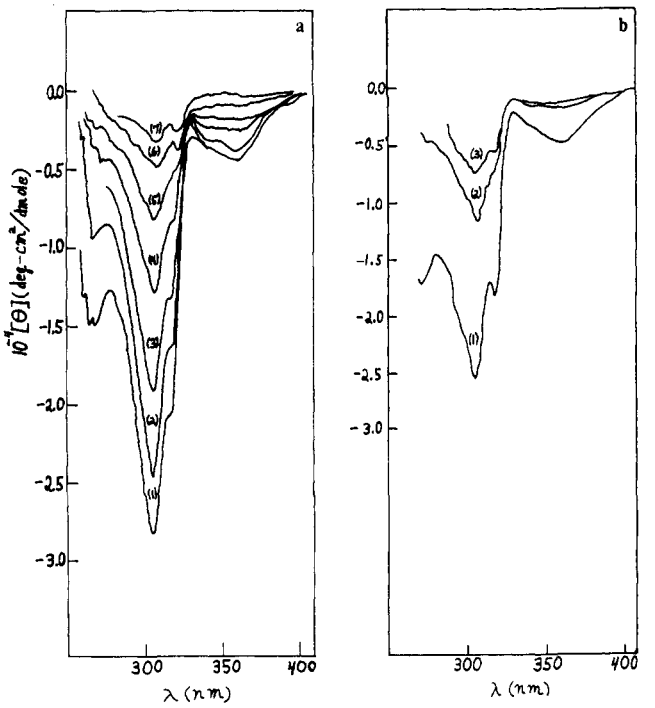

Figure 8. CD spectra, in the chromophore region, of $(Glu)_n$ labeled with **2** at various pHs. (a) Polymer in water at (1) pH 4.1; (2) pH 6.1; (3) pH 6.3; (4) pH 6.4; (5) pH 6.7; (6) pH 7.1; (7) pH 8.2. (b) Polymer in dimethylformamide at (1) nominal pH 3.6; (2) nominal pH 7.8; (3) nominal pH 8.5.

transition. This is shown in Figure 9, where CD spectra are displayed for a $(Glu)_n$ 80% of whose residues were labeled with **1**. Low fractional labeling with **1** results in the usual helix–coil transition, but it is clear from Figure 9 that extensive labeling prevents formation of the random coil: both the backbone region (Figure 9a) and the chromophore (Figure 9b) show essentially complete helix even at a pH as high as 9.0.

Discussion

A. Spin-Labels. 1. Oriented $(Glu)_n$. Splitting of hyperfine lines such as is seen in each spectrum of Figure 1b may arise either from dipolar interaction of the two electrons in the biradical or from g anisotropy. We present here a physical

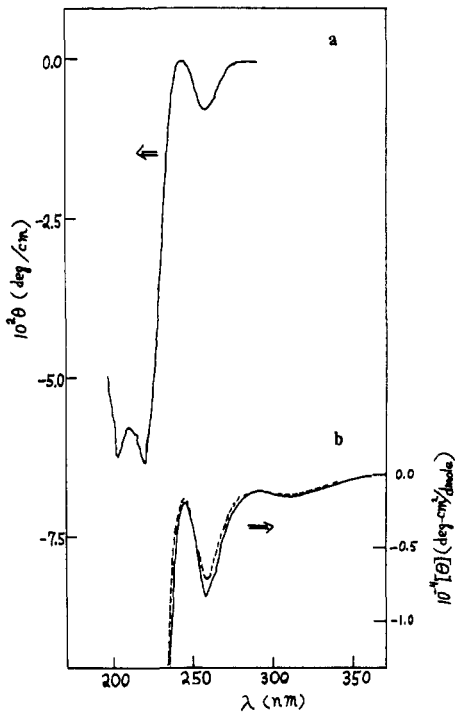

Figure 9. CD spectra of $(Glu)_n$ heavily labeled with **1**. About 80% of the side chains are labeled. (a) Polymer in water at pH 9. Left-hand ordinate gives ellipticity per unit length of a solution containing 3 mg of polymer/100 mL. Both backbone and chromophore regions are shown. (b) Detail of chromophore region. Right-hand ordinate gives molecular ellipticity. Concentration as in a: solid curve, pH 5.4; dashed curve, pH 9.0.

argument that indicates that we cannot at present decide unequivocally which effect, if either, dominates. However, it will become clear below that *g* anisotropy is the more likely possibility.

Of course, we do not know enough about the molecular structure of the labeled film to specify the orientation of each biradical with respect to the *C* axis in the sample. For that reason, we consider two limiting cases, with the aid of Figure 10. In each case, the line *AB* connects the two unpaired electrons (of a given biradical), which have magnetic dipoles S_1 and S_2, respectively. In case 1, *AB* is perpendicular to the *C* axis of the oriented sample; in case 2, *AB* is parallel to the *C* axis. Within each of these limiting molecular cases are two subcases corresponding to the two experimental conditions employed (see Figure 1b), i.e.: in subcase a the external magnetic field is parallel to the *C* axis, whereas in b it is perpendicular to that axis. The physical quantity of importance is θ, the angle between the direction of the spin magnetic moments (which are along H_0) and the line *AB*.

In case 1a, wherein each $S \perp AB$, the angular part of the spin-dipolar interaction [i.e. $3\cos^2(\theta) - 1$] is independent of rotation about the *C* axis and has the value -1. In case 1b, wherein $S \| AB$, that factor (through θ) is dependent upon rotation of *AB* about *C* (while S_1 and S_2 must remain along H_0). Since such rotation of *AB* would come about by rotation of a given, labeled helical molecule about its own cylindrical axis (which is parallel to *C*), which would surely be greatly hindered in the aligned film, the simplest reasonable model for this case would appear to be a static ensemble of molecules, covering the full range of θ without preference. For that model, the average of $3\cos^2(\theta) - 1$ is 2. Thus, in case 1, the splitting produced by the dipolar interaction is expected to be twice as large with $C \perp H_0$ as with $C \| H_0$. Since this is in the same direction as the experimental finding, it would appear that if $AB \perp C$, then the dipolar interaction *could* be the dominant interaction.

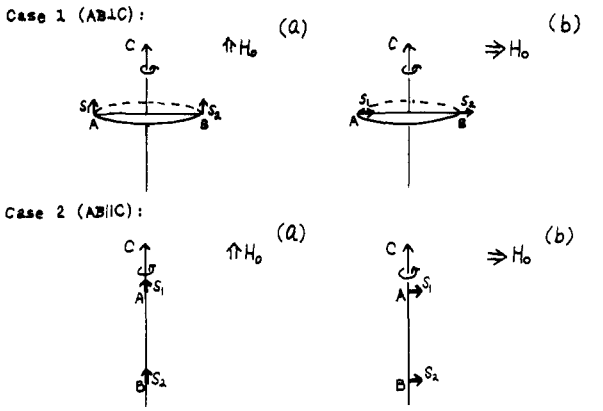

Figure 10. Diagrams illustrating various cases considered in the text. Double arrow gives orientation of the external magnetic field. Arrows S_1 and S_2 represent the two magnetic dipoles of a given biradical label, located, respectively, at A and B in each diagram. Long vertical arrow in each diagram is the *C* axis of the film.

Proceeding to case 2, we find that in case 2a, $3\cos^2(\theta) - 1$ is equal to 2 and in case 2b it is -1. Thus, in case 2, unlike case 1 and unlike the experimental finding, the experimental condition $C \| H_0$ produces twice the dipolar splitting of the condition $C \perp H_0$. Thus, if $AB \| C$, then the dipolar interaction cannot be dominant.

Two further arguments may be brought to bear on this interpretational dilemma. Firstly, the experiments of Glarum and Marshall[16] on diesters of 2,2,6,6-tetramethyl-4-piperidinyl-1-oxy with carbonate, oxalate, etc., indicate that in liquid crystalline media the two free-radical moieties on a given diradical molecule normally assume positions of maximum separation. In those of their compounds most analogous to ours, this means separations of ~15 Å. On this basis alone, we would assume that dipolar interactions are probably not strong.

Secondly, Falle et al.[17] report on biradicals that, in liquid crystalline media in which the long molecular axis is parallel to the field, the three sharp hyperfine lines characteristic of the isotropic spectrum are each split by the same amount because of the dipolar interaction. Reference to Figure 10 shows that this molecular alignment corresponds to case 1b and therefore to the solid curve spectrum (i.e., $H_0 \perp C$) of Figure 1b. Note, however, that although Figure 1b shows splitting in each of three peaks, the amount in the high-field peak is much larger than in the other two. This suggests a different etiology in our case than in that of Falle et al.; i.e. it casts doubt on dipolar interaction as the cause of splitting in our case.

To test the last conclusion, we performed a few experiments on the label itself in a smectic phase made from a 50:50 (w/w) mixture of 4-*n*-pentyloxybenzylidene-4′-aminoacetophenone and 4-*n*-hexyloxybenzylidene-4′-aminoacetophenone. The isotropic mixture was cooled in easy stages from a temperature of 120 to 40 °C in the magnetic field, resulting in a smectic phase in which the long molecular axis is parallel to the field.[18] The resulting ESR spectrum is shown in Figure 11a. If the ESR cell is rapidly turned by 90°, molecular realignment is slow and so spectra may be taken with the long molecular axis perpendicular to the field as well; such a spectrum is shown in Figure 11b. The marked difference in the two spectra clearly proves that there is, indeed, very substantial alignment of the radical molecules. Furthermore, examination of the parallel case (Figure 11a), which corresponds to the alignment in the work of Falle et al., reveals that the three peaks are assuredly not equally split.

We are thus led to state, albeit tentatively, that the intraradical dipolar interactions are not dominating our spectra. Furthermore, since exchange in the label itself (Figure 1a) is

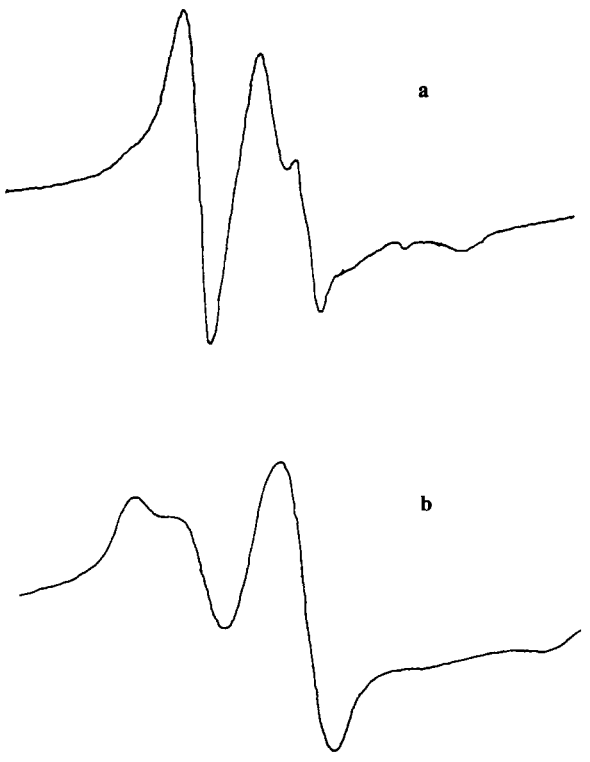

Figure 11. ESR spectra of *cis*-Pt(ATMPO)$_2$(NO$_3$)$_2$ in smectic liquid crystalline phase (see text); temperature 40 °C. (a) Long molecular axis parallel to H_0. The substantial sharp line on the leading edge of the central peak and the small sharp line on the high-field peak are probably due to residual isotropic component, since at 50 °C they were much more prominent and showed the characteristic isotropic splitting. (b) Long molecular axis perpendicular to H_0.

modest and is not visible at all in attached labels where anisotropic motions are not contributing (Figure 4), it seems unlikely that such exchange contributes very much to any of our experiments. At present, therefore, we hypothesize, although with every possible bold-type caveat, that the specifically biradical character of the label is immaterial in interpretation of all our spectra; i.e. that the intralabel dipolar and exchange interactions are not crucial. Needless to say, synthesis of a monoradical analogue of *cis*-Pt(ATMPO)$_2$(NO$_3$)$_2$ and subsequent experimentation would settle the question.

For the present, then, we ascribe the observed ESR splittings in the oriented specimens to the coexistence in the sample of strongly aligned regions (showing g anisotropy) and more isotropic regions. That g anisotropy can lead to effects of the proper magnitude seems clear from very careful experiments and detailed simulations done by Hwang et al.[19]

2. Polypeptides in Solution. Wee and Miller used ATMPO as a primary amine initiator to prepare poly(benzyl-L-glutamate).[4] Each polymer molecule thus synthesized bears a spin-label attached to its end. Although this label is monofunctional, its amino hydrogen can participate in hydrogen bonding with the backbone of the polymer. The resulting loss of flexibility produces an ESR spectrum in marked contrast to the isotropic spectra obtained by side-chain attachment of a monofunctional label. The marked similarity of the spectrum of our *side-chain labeled* (Glu)$_n$ in dimethylformamide (Figure 1c) to that observed by Wee and Miller suggests immediately that the [*cis*-Pt(ATMPO)$_2$]$^{2+}$ label is rather rigidly bound to helical segments of the polymer and that the spectrum therefore contains information about the segmental mobility of the polymer. The most obvious hypothesis that can serve to explain the results of the attachment is that our label is *bifunctionally* attached by chelation of the Pt of the label by adjacent carboxylates of the polymer.

The use of the word "adjacent" above is deliberately vague. We cannot as yet be sure whether the two adjacent carboxylates are n and $n \pm 1$, i.e. a pair "adjacent" as one proceeds along the backbone, or n and $n \pm 4$, i.e. a pair "adjacent" as one proceeds along the axis of the helix. At present we tend to favor the former, since, as noted above, we find no difference in ESR spectra (taken under the same conditions) between samples labeled in the helix state and in the coil state.

The spectrum of helical (Glu)$_n$ in a mixture of water and dimethylformamide (Figure 3b) shows a slow-motion component similar to that in pure dimethylformamide, indicating, again, that the label is responding to the rigidity of the macromolecular helix to which it is attached. Indeed, comparison with the spectrum of the random coil form (Figure 3a) clearly shows the influence of increased backbone flexibility.

The spectra of (Glu)$_n$ in purely aqueous media (Figure 2) reveal further facets of the system. Not even the spectrum of the random coil (Figure 2a) is that of a free spin: the transition to ~50% helix (Figures 2a,b) is accompanied by a small spectral change, the transition from there to full helix (Figures 2b,c) by a bigger change, and the aggregation (Figures 2c,d) by a still bigger change.

The spectrum of (Asp)$_n$ (Figure 4c), unlike that of (Glu)$_n$, shows only loose spins. We interpret this to mean that the labels on (Asp)$_n$ are either single anchored or double anchored on random-coil segments or nonneighboring side chains. Indeed, examination of CPK models confirms this view. It is barely possible, with the shorter side chains of (Asp)$_n$, to chelate the nth and the $n \pm 1$th side chains in the random coil and quite impossible in the helix. Such is not the case in (Glu)$_n$.

Likewise, the spectrum of labeled (Lys)$_n$ shows only weakly immobilized spins, and in this case the interpretation is ambiguous. It is not clear whether binding is bidentate, the extra freedom resulting from the longer side chains in (Lys)$_n$, or monodentate, the extra freedom resulting from rotation about a single bond to the Pt.

Thus, the bifunctional attachment of this platinum compound to side chains in (Glu)$_n$ produces a labeled polymer whose ESR spectrum is sufficiently sensitive to backbone segmental rigidity to reveal clearly and qualitatively the helix–coil transition and polymer aggregation. This probe presumably could be exploited to obtain more quantitative information on those processes. Furthermore, application of this technique need not be confined to polypeptides. Preliminary experiments indicate promise of a similar utility for binding to synthetic polynucleotides and to DNA.[6,20]

B. Chromophore-Labels. If, as seems clear from the experiments on extensive labeling reported in the Results section, bonding of the label stabilizes the helix, then this should be apparent when the helix–coil transition is followed at a low extent of labeling. One would expect, as one sweeps through the transition, that the ellipticity at a wavelength in the backbone region (which monitors the conformation of the bulk of the molecule) would vary nonlinearly with the ellipticity at a wavelength in the chromophore band (which monitors the conformation of the *labeled* residues). Figure 12 confirms this expectation. The ellipticity at the strong backbone peak at 220 nm is well known to be linear in overall helix content, but the plot of $[\theta]_{306}$ (the molecular ellipticity in the chromophore region) vs. θ_{220} is markedly nonlinear; in fact, Figure 12 shows that $[\theta]_{306}$ remains at essentially the same full-helix value until most of the molecule, as judged by θ_{220}, has been converted to random coil. Clearly, the label itself stabilizes the helical conformation of those residues to which it is attached. This immediately argues that binding of Pt cannot be to the polymer backbone, but must be to side chains.

Since the spin-label results suggest that binding is probably to residues n and $n \pm 1$, however, the helical turn must not be viewed as held together by the chelation itself. Rather, the

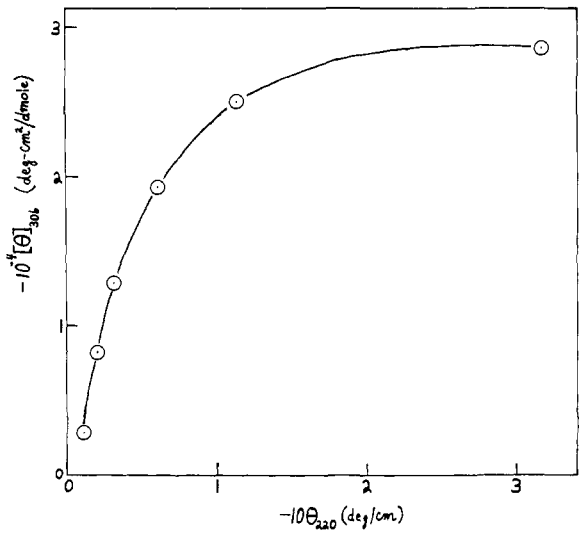

Figure 12. Molecular ellipticity at 306 nm (chromophore region) vs. ellipticity per unit length at 220 nm (backbone region) for $(Glu)_n$ sparsely (~5%) labeled with **2**.

Pt(II) must simply reduce the local charge density and thus produce the extra stability.

The conclusion reached in the preceding section that cis Pt(II) compounds attach to $(Glu)_n$ bifunctionally is thus fully supported by these experiments with chromophore labels. Firstly, the similarity of the UV spectra of labeled $(Glu)_n$ to labeled oxalate is certainly suggestive. Secondly, the absence, in labeled $(Glu)_n$, of spectral shifts characteristic of OH^- binding to Pt, which are clearly observed for label alone, points conclusively to the idea that both of the two ligand positions not occupied by aromatic nitrogens are occupied by polymer carboxylates.

The precise physical origins of the induced CD are very difficult to specify. However, a few tentative suggestions may prove heuristic. The chromophores themselves are symmetric, so clearly their interaction with the dissymmetric polymer produces the CD. In accord with this, a few experiments done with labeled $(D\text{-}Glu)_n$ produced CD spectra the mirror image of those shown here.[6] Furthermore, chromophore-chromophore interactions on the polymer are not significant since the CD spectrum at low extent of labeling is independent of the extent of labeling. Finally, the absence of CD in the chromophore band for labeled random coil and for labeled sodium glutamate monomers plainly implicates dissymmetric perturbation of the chromophore by the helical structure itself rather than by, say, the dissymmetric backbone α carbon. We next conjecture how this perturbation might come about.

A theory has been developed describing CD that is induced in groups attached to a polymer; the equations involve the dot products of the various transition electric dipole moments with the other transition electric dipole moments in the system (the "μ-μ" mechanism) and with the other transition magnetic dipole moments in the system (the "μ-m" mechanism).[21] In the present instance, we are concerned with the π-π^* ($^1B_1$) band of the chromophore label, a band which is essentially magnetic dipole forbidden. Hence, the only relevant terms become those involving coupling of the chromophore electric dipole transition moment with magnetic and electric transition moments of other relevant groups. Since the polymer backbone is rather distant from the chromophore, the perturbing groups most likely to be significant are the chelating carboxylates. The n-π^* transition of the carboxylates is magnetic dipole allowed and might conceivably couple with the electric transition dipole of the chromophore. However, the two transitions are rather well separated in energy (carboxylate n-π^* is at ~200 nm,

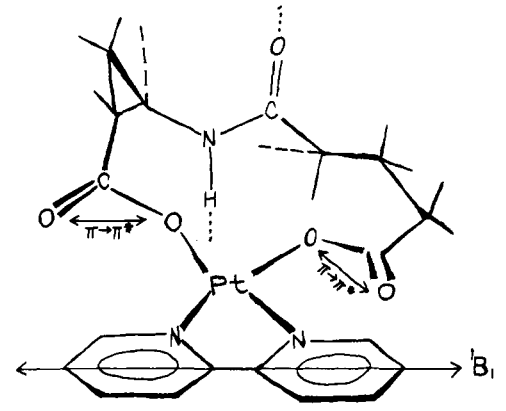

Figure 13. Diagram showing geometry of chelation of adjacent side chains of helical $(Glu)_n$ by **2**. Dotted lines indicate hydrogen bonding in the backbone. Dashed lines show covalent bonds to rest of polymer chain. Directions of transition moments of the $^1B_1$ chromophore band and π-π^* carboxylate bands are indicated.

whereas chromophore $^1B_1$ lies at 300–330 nm), suggesting only a small contribution. The interaction of the π-π^* transition electric dipole of the carboxylates with that of the chromophore therefore suggests itself as the dominant mechanism.

The diagram of Figure 13 shows the spatial relationship of the relevant transition electric dipoles. We have made CPK models of $(Glu)_n$ segments with attached **2** and it is clear that there are only a few possible conformational forms of the resulting chelated ring and that interconversion from one form to another is not possible so long as the segment stays helical. Nor is it likely that, in any of the possible ring conformations, any of the dot products of the transition electric dipole moments are near zero. The flexible structure of the random coil form, however, not only allows interconversion of these few conformations of the chelated ring, but makes possible numerous intermediate conformations as well, a circumstance that may well cause the dot product of the transition moments to average to near zero. We thus suggest, albeit tentatively, that the CD induced in the chromophore label by attachment to the helix arises because the rigidity of the resulting ring leads to a substantial coupling between the transition electric dipoles of the $^1B_1$ chromophoric transition and the π-π^* transition of the polymer carboxylates, a coupling that averages to near zero in the random coil polymer conformation.

Acknowledgment. We wish to thank Professor Samuel Weissman for several very enlightening discussions of the ESR data, especially in connection with the averaging appropriate to case 1b of Figure 10. We also acknowledge a critical analysis, by Professor Wilmer Miller, of an earlier version of this paper that led to important changes. Dr. Pu-Sen Wang provided vital input in connection with the experiment in smectic liquid crystals.

References and Notes

(1) This investigation was supported by Research Grant No. GM-20064 from the Division of General Medical Sciences, U.S. Public Health Service.
(2) Address correspondence to this author at the Department of Chemistry, Washington University.
(3) P. L. Nordio, A. Scatturia, and A. M. Tamburro, *Ric. Sci.*, **38**, 832 (1968).
(4) E. L. Wee and W. G. Miller, *J. Phys. Chem.*, **77**, 182 (1973).
(5) Y.-Y. H. Chao and A. Holtzer, *Biochemistry*, **14**, 1264 (1975).
(6) Y.-Y. H. Chao, Ph.D. Thesis, Washington University, St. Louis, Mo., 1975.
(7) G. B. Kauffman, *Inorg. Synth.*, **7**, 250 (1963).
(8) P. Saludjian, C. deLoze, and V. Luzzati, *C. R. Hebd. Seances Acad. Sci.*, **265**, 4514 (1963).
(9) R. P. Mason, C. F. Polnaszek, and J. H. Freed, *J. Phys. Chem.*, **78**, 1324 (1974).
(10) M. Nagasawa and A. Holtzer, *J. Am. Chem. Soc.*, **86**, 538 (1964).
(11) E. König and H. L. Schläfer, *Z. Phys. Chem. (Frankfurt am Main)*, **26**, 371 (1960).
(12) Y. Gondo, *J. Chem. Phys.*, **41**, 3928 (1964).

(13) S. F. Mason, *Inorg. Chim. Acta Rev.*, **2**, 89 (1968).
(14) R. G. Bray, J. Ferguson, and C. J. Hawkins, *Aust. J. Chem.*, **22**, 2091 (1969).
(15) E. Beilli, P. M. Gidney, and B. T. Heaton, *J. Chem. Soc., Dalton Trans.*, 2133 (1974).
(16) S. Glarum and J. Marshall, *J. Chem. Phys.*, **47**, 1374 (1967).
(17) H. R. Falle, G. Luckhurst, H. Lemaire, Y. Marechal, A. Rassat, and P. Rey, *Mol. Phys.*, **11**, 49 (1966).
(18) Pu-Sen Wang, personal communication.
(19) J. S. Hwang, R. Mason, L.-P. Hwang, and J. Freed, *J. Phys. Chem.*, **79**, 489 (1975).
(20) S. H. Mastin, unpublished work; a brief summary of some of this work has been given in Varian Application Note EPR-75-1 of March, 1975.
(21) I. Tinoco, *Adv. Chem. Phys.*, **4**, 113 (1961).

Oxidation and Reduction of Iron Porphyrins and Hemoproteins by Quinones and Hydroquinones

C. E. Castro,* G. M. Hathaway, and R. Havlin

Contribution from the Department of Nematology, University of California, Riverside, California 92521. *Received February 3, 1977*

Abstract: High-spin iron(II) porphyrins in *N*-methylpyrrolidone-acetic acid, methanol, or benzene are very rapidly oxidized by quinones at room temperature. The corresponding iron(III) porphyrins and hydroquinones are the only products. The reaction is *not* reversible. The oxidation is inhibited by amine ligands that impart a low-spin state. The corresponding low-spin adducts are inert to benzoquinone in the absence of a proton source. The hexacoordinate low-spin species are, however, oxidized by an outer sphere mechanism that is acid dependent. NMR and visible spectra of the low-spin adducts and the influence of axial ligands upon the rates of oxidation are consistent with a rate-limiting step that entails dissociation of a protonated 1:1 iron porphyrin-quinone π complex. The redox reaction of the low-spin complexes is reversible, and reduction by hydroquinone is also an outer sphere process. The pattern of the influence of axial ligand upon the rate of oxidation and reduction of the low-spin complexes by quinone and hydroquinone is the same. The rate of both processes increases with expected metal-porphyrin d-π interaction in the various complexes. The results indicate two mechanisms for the oxidation of iron(II) porphyrins that are dependent upon axial ligation and spin state. High-spin (presumably) pentacoordinate hemes are oxidized by an axial inner sphere process, the low-spin hexacoordinate species by a peripheral π transfer. The reduction of these latter occurs by a similar mechanism. The reactivity of the iron(II) and iron(III) proteins myoglobin and cytochrome *c* to these reagents matches the reactivity of the corresponding iron porphyrins and accords well with theory. Hydroquinone is a specific probe for the peripheral π-transfer capacity of hemoproteins in solution.

Quinones and hydroquinones may play an important role in the electron-transport sequence[1] manifest in mitochondria. Moreover, quinones are one of the bond types noted to oxidize high-spin iron(II) porphyrins in homogeneous solution.[2] As a follow-up to these initial findings, we report here our studies of the oxidation and reduction of iron porphyrins by quinones and hydroquinones. The work is a part of our effort to develop the organic redox chemistry of these iron units such that mechanistically defined reagents may be used as substrates to plumb the influence of a protein upon the reactivity of its heme in a variety of hemoproteins. Our general approach has been summarized, and a brief account of a portion of the quinone work has been presented.[3]

Results

Stoichiometry. (a) High-Spin Iron Porphyrins. Solutions of deuteroheme in 1:1 v/v *N*-methylpyrrolidone-acetic acid[7,19] were employed as primary scanning reagent. The visible spectrum of the iron(II) complex (λ_{max} 540 nm) is typical of a high-spin heme.[4] A wide array of quinones were examined for oxidative reactivity. All quinones oxidized the heme rapidly at room temperature in this solvent, benzene (containing 1–2% acetic acid), or methanol. The stoichiometry (eq 1) was established for benzoquinone in methanol by direct spectral observation of the hydroquinone at 246–250 nm and by flame ionization gas chromatography. The reaction is quantitative. Generally, it was not possible to gas chromatograph the air-sensitive hydroquinone products, and visible spectral verification was also beclouded by the spectra of the iron(II) and iron(III) porphyrin. Consequently, many of the hydroquinone products could be demonstrated only by direct thin-layer chromatography of the reaction mixture under nitrogen (cf. the Experimental Section). In all cases, the conversion of iron(II) to iron(III) porphyrin was quantitative and, except for the porphyrins, no organics except the quinone and hydroquinone were visible in the product mixture. Table I lists the quinones examined. In no case, including ubiquinone or vitamin K_1, did the reverse reaction occur.

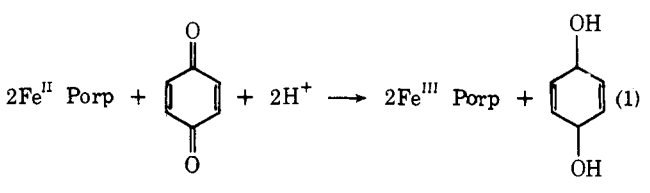

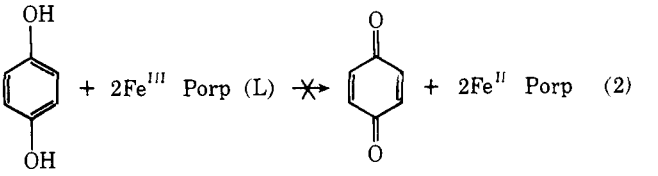

L = MeOH, Cl^-, OAc^-

We conclude *high-spin iron(III) porphyrins* **are not** *reduced by* hydroquinones at room temperature, and this accords with estimates of the overall thermodynamics (see below). The quinone-hydroquinone pair was used to further plumb the influence of porphyrin, axial ligand, and solvent on these reactions.

(b) Low-Spin Iron Porphyrins. In contrast to the behavior exhibited by the high-spin iron complexes, their low-spin counterparts in pyridine are cleanly reduced to the iron(II)